

## Dielectrophoretic assembly of reversible and irreversible metal nanowire networks and vertically aligned arrays

S. J. Papadakis<sup>a)</sup>

*Johns Hopkins University Applied Physics Laboratory, 11100 Johns Hopkins Road, Laurel, Maryland 20723*

Z. Gu

*Department of Chemical and Biomolecular Engineering, Johns Hopkins University, 3400 North Charles Street, Baltimore, Maryland 21218*

D. H. Gracias

*Department of Chemical and Biomolecular Engineering, and Department of Chemistry, Johns Hopkins University, 3400 North Charles Street, Baltimore, Maryland 21218*

(Received 6 January 2006; accepted 19 April 2006; published online 9 June 2006)

We demonstrate the dielectrophoretic control of metallic nanowires (NWs) in liquid suspensions. By varying a range of parameters including the magnitude and frequency of the applied electric field, the liquid suspending the NWs, and the flow conditions, we demonstrate control over NW network formation and dissolution, as well as ordering of NWs into vertically aligned arrays. These results suggest a straightforward strategy for NW assembly and integration in devices. © 2006 American Institute of Physics. [DOI: 10.1063/1.2209174]

Electrodeposition into nanoporous templates is an inexpensive and massively parallel fabrication technique for nanowires (NWs).<sup>1,2</sup> Since a wide range of metals and semiconductors can be electrochemically deposited, templated electrodeposition allows the fabrication of NW-based electronic components including conductors, resistors, and diodes.<sup>3</sup> However, in order to integrate NW-based devices with complementary metal-oxide semiconductor (CMOS) and microelectromechanical system (MEMS) technologies, strategies must be developed to precisely position NWs on microfabricated contact pads. Prior studies have demonstrated the directed assembly of NWs using magnetic,<sup>4,5</sup> ligand receptor,<sup>6</sup> and surface tension assembly.<sup>7</sup> Dielectrophoresis<sup>8–17</sup> (DEP) is also a promising directed-assembly technique to integrate NWs with substrates since both the NW alignment and placement are controlled.<sup>10,14,16–18</sup> In contrast to other techniques, DEP is extremely versatile (since most materials are polarizable and DEP requires no surface functionalization) and DEP can be scaled to the wafer level, making large scale manufacturing feasible.

In this letter we describe the dielectrophoretic control of metal NWs resulting in reversible or irreversible end-to-end networks and branched networks, and a remarkable vertical alignment of NWs on top of patterned electrodes. The experimental results include the assembly of extended NW networks as opposed to single-NW interconnects, the tuning of the adhesion between the NWs and the substrate resulting in control over the reversibility of the NW network assemblies, insight into the factors that determine the degree of branching in DEP-assembled networks, and the effects of electroosmotic flow which aids the vertical alignment of the NWs on substrates. These results demonstrate the potential for the highly parallel fabrication of NW devices in a range of electronic, photonic, and biomedical applications. For example, sparse end-to-end NW networks are promising for electronic

devices due to the small number of NW junctions within the network, densely branched NW networks are advantageous for use as sensors due to their large surface area to volume ratios,<sup>19</sup> and vertically aligned NW arrays can function as vertical interconnects in damascene integration of microelectronic devices,<sup>20</sup> as switchable obstacle filters in microfluidics, and as gratings that can be assembled on demand in nanophotonic devices.

Silver (Ag) and gold (Au) NWs with lengths of 4–5  $\mu\text{m}$  were grown in templates with nominal pore diameters of 200 and 50 nm as described previously, and subsequently suspended in a solvent.<sup>5,7</sup> Sinusoidal voltages ranging from 10 Hz to 100 kHz were applied to electrodes (100 nm of Au with a Cr adhesion layer) lithographically patterned on glass substrates. Two configurations were employed: two pointed electrodes facing each other and a pointed electrode facing a flat electrode. A small liquid cell was created above the electrodes using a silicone seal and a glass cover slip. Images were taken using an optical microscope and charge coupled device (CCD) camera.

Using DEP, reversible (Fig. 1) and irreversible [Figs. 2(a) and 2(b)] NW networks were created by an appropriate choice of the solvent in which the NWs were suspended. The solvent affected the adhesion between the substrate and the NWs, and between the NWs themselves. Reversible net-

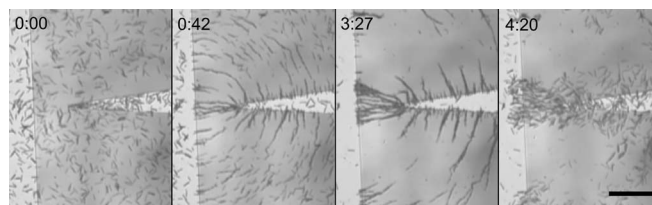


FIG. 1. Reversible Ag nanowire network formation from a suspension in water, with DEP at 0.2 V and 100 kHz (Ref. 21). The frames are labeled with the time (min:s) after the first frame. The first frame is taken just before initiation of DEP, and the third frame is taken just before ending DEP. The scale bar corresponds to 30  $\mu\text{m}$ .

<sup>a)</sup>Electronic mail: stergios.papadakis@jhuapl.edu

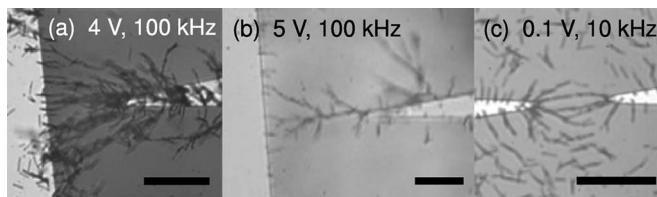


FIG. 2. Examples of nanowire structures formed by dielectrophoresis of nanowires in liquid suspension. (a) Dense, overlapped network (Ref. 21). (b) Sparse, branching network. (c) End-to-end joined, predominately unbranched network. The scale bars correspond to  $30\ \mu\text{m}$ .

works were created in water, where NWs which settled to the substrate did not adhere well and were readily observed undergoing Brownian motion. The network in Fig. 1 was created in a sealed cell by letting the NWs settle and then applying  $0.2\ \text{V}$  at  $100\ \text{kHz}$  across the electrodes. The network was disrupted by Brownian motion when the voltages were turned off.

In contrast, in ethanol the NWs adhered to the substrate and no Brownian motion was evident. Since DEP forces were insufficient to overcome the adhesion of the NWs to the substrate, a flowing ethanol/NW suspension was used to bring a constant supply of NWs within range of the electric field (E-field) gradients between the electrodes [Fig. 2(a)]. Once collected by DEP, the NWs adhered strongly enough to the substrate to withstand the flow and the NW network remained intact after DEP was discontinued. This network formation process is irreversible. It should be noted that the networks were disrupted slightly when the ethanol was evaporated; alternate methods such as supercritical drying may be needed if the disruption is to be minimized.

The adhesion could be tuned by using a mixture of ethanol and water to suspend the NWs. The branching network in Fig. 2(b) was created in sealed cell from a suspension of NWs in 2 parts water and 1 part ethanol. Before DEP was started, all of the visible NWs exhibited Brownian motion, indicating that they had not adhered to the surface. When the E-fields were applied, the network assembled. After the E-fields were turned off, those NWs which were part of the network and those which were on the edges of the electrodes adhered to the substrate, while those in the center of the electrodes or farther away on the glass resumed their Brownian motion.

We attribute the differences in adhesion to a combination of electrostatic repulsion, surface tension, and van der Waals (vdW) forces. In water, we believe that electrostatic double layer forces prevented direct contact of NWs to the substrate resulting in weak adhesion. Ethanol, which is much less polar, did not prevent the NWs from sticking to the substrate under the force of gravity and vdW forces. In the water/ethanol mixture, the DEP forces in regions of highest E-field gradient were sufficient to allow the vdW forces to take hold irreversibly.

In sealed-cell water and water/ethanol mixture experiments, with NWs settled on the substrate, the network density was limited by the initial density of NWs on the substrate [Figs. 1 and 2(b)] because the local area was depleted of NWs as they formed the network. For networks created from a flowing ethanol suspension, the density was limited by the time for which DEP was performed [Fig. 2(a)].

The amount of branching in the networks was primarily determined by the rate of network formation. For small volt-

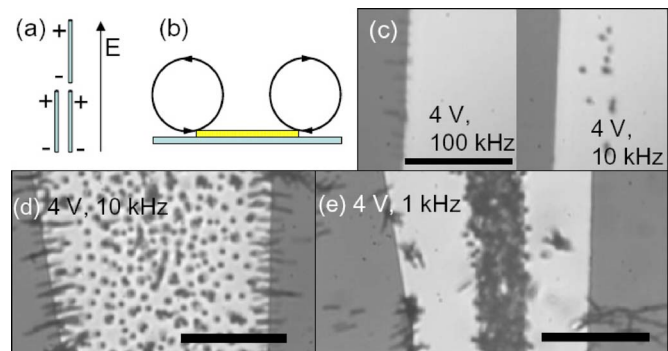


FIG. 3. (Color online) (a) Schematic of induced dipoles in nanowires. (b) Schematic of the circular flow pattern generated at the edges of the electrodes. (c)  $50\ \text{nm}$  diameter nanowires aligned at the edge of the pointed electrode, a few hundred microns from the point, with  $100\ \text{kHz}$  E-fields; then standing vertically on top of it with  $10\ \text{kHz}$  E-fields (the dots are the nanowires seen end on). (d)  $200\ \text{nm}$  diameter nanowires standing on top of the electrode, a few hundred microns from the point. (e) Vertical nanowires pushed towards the center of the electrode by flow. The scale bars correspond to  $30\ \mu\text{m}$ .

age amplitudes of around  $0.2\ \text{V}$ , with electrode spacings of  $25\ \mu\text{m}$ , given starting surface NW densities comparable to those in Figs. 1 and 2(c), networks with few or no branches were formed over tens of seconds. During the formation of these networks, the NW velocities caused by DEP were small compared to the Brownian motion. The negligible momentum of the NWs allowed them to sample different spatial positions in order to find their minimum-energy end-to-end configuration. Voltages greater than  $2\ \text{V}$  resulted in branching networks [Fig. 2(b)]. The NWs approached the network rapidly and did not have time to align with the ends of already-assembled chains, resulting in branches. Conditions of rapid flow also resulted in branches. Moreover, suspensions in water were more likely to form end-to-end networks than suspensions in ethanol or mixtures, since some rearranging was possible after the NW was incorporated into the network.

At voltages greater than  $1\ \text{V}$  and a frequency of  $100\ \text{kHz}$ , if DEP was started before the NWs settled to the substrate, bulk networks which rose from the substrate and assembled in the bulk of the solvent were formed.<sup>11,13</sup> They remained in the bulk tracing the E-field lines. The network in the top part of Fig. 2(b), originating about  $40\ \mu\text{m}$  from the point of the electrode, is a bulk network, recognizable because it rises out of the microscope's focal plane.

By performing DEP at different frequencies in the proper sequence, vertically aligned arrays of NWs were formed (Fig. 3). At  $100\ \text{kHz}$  and larger frequencies, the behavior of the NWs was qualitatively what one would expect from the simplest model for DEP. The NWs aligned with the E-field and moved towards regions of highest E-field, collecting at local maxima. With  $10\ \text{kHz}$  of applied field, we observed a circular flow pattern, centered on the edges of the electrodes, rapid enough to significantly affect the NW behavior [Fig. 3(b)].<sup>15,22,23</sup> We attribute this flow to frequency-dependent ac electro-osmosis, an interaction of nonuniform ac electric fields and surface ionic charges.<sup>22-25</sup> Under electro-osmosis, fluid is driven by the tangential component of the nonuniform E-field in the electrical double layer above the electrodes. The vertically aligned NWs in Figs. 3(c) and 3(d) were generated by first applying a  $4\ \text{V}$ ,  $100\ \text{kHz}$  potential to the electrodes, which collected NWs along the edges of the

electrode and depleted NWs from both the top of the electrode and the surrounding substrate. Then, the frequency was switched to 10 kHz, generating the flow pattern which swept the NWs onto the electrodes. The flow also aided them in aligning vertically with the E-field. NWs which were horizontal on top of the electrodes had very little torque applied because the dipole was induced across the NW diameter, which resulted in a very weak dipole moment aligned with the E-field. When the flow disturbed them from the horizontal position the NWs were no longer perpendicular to the applied E-field, so the induced dipole moment and the angle of the dipole relative to the field were significantly increased, increasing the torque and causing the NWs to stand vertically. When the drive frequency was decreased further to 1 kHz the flow intensified, removing more NWs from the electrode edges and forcing all of the NWs towards the center of the electrode [Fig. 3(e)]. It should be noted that the NWs did not adhere together under these conditions; when the frequency was increased again to 10 kHz, the NWs drifted apart and recovered the distribution of Fig. 3(d). Frequency reduction to 100 Hz intensified the flow enough that the NWs were picked up from the surface and carried in circles.<sup>21</sup>

We also observed that the NWs used in our experiments picked up residual charge either during processing or DEP, as evidenced by the fact that under 10 Hz E-fields, the NW positions oscillated while their average positions slowly moved towards E-field maxima. The mutual repulsion of the NWs due to the charging was weaker than the DEP forces: DEP caused NWs in line with each other attract due to dipolar interactions [Fig. 3(a)], despite any repulsion due to charging. For example, the second panel of Fig. 1 shows NWs away from the electrodes self-assembled end to end. When NWs were aside one another, dipolar interactions caused repulsion: vertically aligned NWs formed roughly equally spaced arrays [Fig. 3(d)], and NWs at electrode edges shifted laterally to make room for other approaching NWs.<sup>21</sup>

The NW diameter had moderate effects on NW behavior. Due to their lower mass and larger surface area to volume ratio, the 50 nm diameter NWs took longer to settle to the bottom of the liquid cell (minutes instead of tens of seconds), exhibited more rapid Brownian motion, and were more affected by flow than the 200 nm NWs. For example, while no 200 nm NWs were carried by the circular flow driven by 10 kHz E-fields, many 50 nm NWs were. Also, since NW polarizability is a much weaker function of diameter than is the mass, 50 nm NWs on top of electrodes were rotated more easily from horizontal to vertical with minimal electroosmotic flow.

To summarize, we have demonstrated scalable techniques whereby NWs can be coaxed to form assemblies that may be useful in a variety of devices. We have investigated only a fraction of the parameter space available for control-

ling NWs in suspension by DEP. Tailored functional surface coatings would allow significant flexibility in tuning the adhesion of NWs to specific locations on the substrate or each other. Suspensions in other liquids, different electrode geometries, and multicomponent NWs with and without surface modifications all could offer additional flexibility and more precise control of NW placement. Finally, it will be necessary to explore strategies to permanently bond vertically aligned NWs so that these assemblies can be used in functional devices.

<sup>1</sup>C. R. Martin, *Science* **266**, 1961 (1994).

<sup>2</sup>A. Huczko, *Appl. Phys. A: Mater. Sci. Process.* **70**, 365 (2000).

<sup>3</sup>S. Park, S.-W. Chung, and C. A. Mirkin, *J. Am. Chem. Soc.* **126**, 11772 (2004).

<sup>4</sup>C. L. Chien, L. Sun, M. Tanase, L. A. Bauer, A. Hultgren, D. Silevitch, G. J. Meyer, P. C. Searson, and D. H. Reich, *J. Magn. Magn. Mater.* **249**, 146 (2002).

<sup>5</sup>H. Ye, Z. Gu, T. Yu, and D. H. Gracias, *IEEE Trans. Nanotechnol.* **5**, 62 (2005).

<sup>6</sup>A. K. Salem, M. Chen, J. Hayden, K. W. Leong, and P. C. Searson, *Nano Lett.* **4**, 1163 (2004).

<sup>7</sup>Z. Gu, H. Ye, and D. H. Gracias, *J. Mater.* **57**, 60 (2005).

<sup>8</sup>T. B. Jones, *Electromechanics of Particles* (Cambridge University Press, Cambridge, New York, 1995).

<sup>9</sup>H. A. Pohl, *Dielectrophoresis: The Behavior of Neutral Matter in Nonuniform Electric Fields* (Cambridge University Press, Cambridge, New York, 1978).

<sup>10</sup>P. A. Smith, C. D. Nordquist, T. N. Jackson, T. S. Mayer, B. R. Martin, J. Mbindyo, and T. E. Mallouk, *Appl. Phys. Lett.* **77**, 1399 (2000).

<sup>11</sup>K. Hermanson, S. Lumsdon, J. Williams, E. Kaler, and O. Velev, *Science* **294**, 1082 (2001).

<sup>12</sup>A. Docoslis and P. Alexandridis, *Electrophoresis* **23**, 2174 (2002).

<sup>13</sup>K. H. Bhatt and O. D. Velev, *Langmuir* **20**, 467 (2004).

<sup>14</sup>S. Evoy, N. DiLello, V. Deshpande, A. Narayanan, H. Liu, M. Riegelman, B. Martin, B. Hailer, J.-C. Bradley, W. Weiss, T. Mayer, Y. Gogotsi, H. Bau, T. Mallouk, and S. Raman, *Microelectron. Eng.* **75**, 31 (2004).

<sup>15</sup>Y. J. Yuan, M. K. Andrews, and B. K. Marlow, *Appl. Phys. Lett.* **85**, 130 (2004).

<sup>16</sup>J. J. Boote and S. D. Evans, *Nanotechnology* **16**, 1500 (2005).

<sup>17</sup>L. Dong, J. Bush, V. Chirayos, R. Solanki, J. Jiao, Y. Ono, J. F. Conley, Jr., and B. D. Ulrich, *Nano Lett.* **5**, 2115 (2005).

<sup>18</sup>D. L. Fan, F. Q. Zhu, R. C. Cammarata, and C. L. Chien, *Phys. Rev. Lett.* **92**, 247208 (2005).

<sup>19</sup>D. Zhang, Z. Liu, C. Li, T. Tang, X. Liu, S. Han, B. Lei, and C. Zhou, *Nano Lett.* **4**, 1919 (2004).

<sup>20</sup>J. Li, Q. Ye, A. Cassell, H. T. Ng, R. Stevens, J. Han, and M. Meyyappan, *Appl. Phys. Lett.* **82**, 2491 (2003).

<sup>21</sup>See EPAPS Document No. E-APPLAB-88-202623 video clips of the assembly of the networks in all three figures, and a video clip of repulsion of NWs parallel to each other. All of the video clips can be accessed by opening file index.html. This document can be reached through a direct link in the online article's HTML reference section or via the EPAPS homepage (<http://www.aip.org/pubservs/epaps.html>).

<sup>22</sup>A. Ramos, H. Morgan, N. Green, and A. Castellanos, *J. Phys. D* **31**, 2338 (1998).

<sup>23</sup>N. Green, A. Ramos, A. Gonzalez, H. Morgan, and A. Castellanos, *Phys. Rev. E* **66**, 026305 (2002).

<sup>24</sup>A. Ramos, H. Morgan, N. Green, and A. Castellanos, *J. Colloid Interface Sci.* **217**, 420 (1999).

<sup>25</sup>N. Green, A. Ramos, and H. Morgan, *J. Phys. D* **33**, 632 (2000).